

Topological insulator and particle pumping in a one-dimensional shaken optical latticeFeng Mei,^{1,2,*} Jia-Bin You,² Dan-Wei Zhang,³ X. C. Yang,³ R. Fazio,^{2,4,†} Shi-Liang Zhu,^{1,‡} and L. C. Kwek^{2,5,6,§}¹*National Laboratory of Solid State Microstructures, Department of Physics, Nanjing University, Nanjing, China*²*Centre for Quantum Technologies, National University of Singapore, 3 Science Drive 2, Singapore 117543, Singapore*³*Laboratory of Quantum Information Technology and SPTE, South China Normal University, Guangzhou 510006, China*⁴*NEST, Scuola Normale Superiore and Istituto Nanoscienze-CNR, I-56126 Pisa, Italy*⁵*Institute of Advanced Studies, Nanyang Technological University, 60 Nanyang View, Singapore 639673*⁶*National Institute of Education, Nanyang Technological University, 1 Nanyang Walk, Singapore 637616*

(Received 21 October 2014; published 29 December 2014)

We propose a simple method to simulate and detect topological insulators with cold atoms trapped in a one-dimensional bichromatic optical lattice subjected to a time-periodic modulation. The tight-binding form of this shaken system is equivalent to the periodically driven Aubry-Andre model. We demonstrate that this model can be mapped into a two-dimensional Chern insulator model, whose energy spectrum hosts a topological phase within an experimentally accessible parameter regime. By tuning the laser phase adiabatically, such one-dimensional system constitutes a natural platform to realize topological particle pumping. We show that the Chern number characterizing the topological features of this system can be measured by detecting the density shift after one cycle of pumping.

DOI: [10.1103/PhysRevA.90.063638](https://doi.org/10.1103/PhysRevA.90.063638)

PACS number(s): 67.85.-d, 03.75.Ss

I. INTRODUCTION

Since the discovery of topological insulators, the search for a topological state of matter has attracted intense interest in past years in condensed-matter physics [1,2] and atomic, molecular, and optical physics [3]. One of the recent theoretical advances in this field is the introduction of Floquet topological insulators [4–10]. It is shown that a topological trivial system can become nontrivial in the presence of time-periodic perturbations. The classification of Floquet topological insulator is based on analyzing the properties of the Floquet operator [11,12]. In particular, these periodic perturbations could be easily achieved by externally shining laser fields on the system with microwave frequencies [4–10]. However, in a solid-state system, the materials with topological features are still quite scarce and the tools to engineer the topological phase remain limited.

Ultracold atoms trapped in an optical lattice nowadays have been widely recognized as powerful tools to simulate and study many-body problems originally from condensed-matter physics [13,14]. This arises from the fact that the cold atomic systems can provide a clean platform without lattice disorder and even some extreme physical situations unachieved in condensed-matter physics can be reached here. Experimentally, great progress has been achieved recently in realizing artificial gauge fields [15–18], spin-orbit coupling for ultracold atoms [19–21], and spin Hall effects [22], which turn cold atoms into a new platform for simulating topological phases. Some proposals have been put forward to use this system to mimic quantum anomalous Hall insulators (Chern insulators) [23–27], time-reversal-invariant topological insulators [28,29], and Majorana fermions [30]. In particular,

cold atoms in modulated optical lattices constitute a versatile platform to realize synthetic gauge fields and topological phases [31]. For instance, such setups have been considered recently to experimentally realize the Haldane [23,25,32] and the Hofstadter model [33], using the technology of modulated optical lattices [34,35]. These experiments led to the first experimental determination of the Chern number using cold atoms [35].

Remarkably, recent studies have also shown that some topological properties of the two-dimensional (2D) integer quantum Hall insulator could be simulated with a one-dimensional (1D) Aubry-Andre (AA) model [36]. When the 1D model depends on a parameter in a periodic manner, one can regard this system as a 2D system, where the physical dimension is extended by the 1D parameter space. Then the topological property of this system can be characterized by the Chern number defined on a torus formed by a spatial dimension as well as a parameter dimension. For a cold atomic system, the AA model has been experimentally realized in a 1D optical lattice for studying Anderson localization [37] and recently been discussed for simulating quantum Hall insulator [38,39] and topological bosonic Mott insulator [40,41] and charge pumping [42]. This idea has also been generalized to realize the Haldane insulator with a 1D extended Su-Schrieffer-Heeger model [43]. Compared with the previous methods for realizing topological phase, the present method does not need the engineering of synthetic gauge fields, which provides an alternative simple route to probe the topological feature of quantum Hall states. Another route is also offered by the so-called synthetic dimensions, which use the internal states of the atoms [44].

In this paper, we take one step further and show that the AA model can have the same topological feature as the 2D Chern insulator, when it is subjected to periodic drive. The 2D Chern insulator is different from the standard quantum Hall insulator, as it does not require a magnetic field to break time-reversal symmetry, and thus it does not display Landau levels. Its discovery stimulated the search for different exotic topological

*tianfengmei@gmail.com

†r.fazio@sns.it

‡slzhu@nju.edu.cn

§cqtklc@nus.edu.sg

phases, including a Z_2 topological insulator and a topological superconductor [1,2]. In this paper, we focus on its realization using cold atoms trapped in a 1D shaken bichromatic optical lattice, but we note that it can also be achieved in 1D quasicrystal systems [45]. When the lattice modulation is in the high-frequency regime, we find that the energy spectrum associated with the effective time-independent Hamiltonian displays a gapped Chern insulator phase. In contrast to the recent proposals for realizing a Floquet topological insulator in a 2D optical lattice [31], one of the advantages of this 1D framework is that topological pumping arises naturally. This pumping is topologically protected because the 1D model shares the same topological origin as the 2D Chern insulator. The number of pumped particles can be expressed as the Chern number of this system. Then we employ such pumping to detect the Chern number, hence characterizing the topological property of the system.

The paper is organized as follows. Section II introduces the periodically driven AA model, which can be realized with ultracold atoms trapped in a shaken bichromatic optical lattice. Section II presents the effective Hamiltonian of the periodically driven AA model. In Sec. III, we study some topological features of the system, such as Chern number and edge states. In Sec. V, we present a feasible approach to detect the topological Chern number based on topological pumping. A short conclusion is given in Sec. VI.

II. PERIODICALLY DRIVEN AA MODEL

We consider ultracold fermionic atoms trapped in a shaken bichromatic optical lattice. This lattice is generated by the superposition of two shaken optical lattices. The single-particle Hamiltonian of an atom in this shaken lattice system is written as

$$H_s = \frac{p_x^2}{2M} + V_1 \sin^2[k_1(x - x_1(t))] + V_2 \sin^2[k_2(x - x_2(t) + \phi/2)], \quad (1)$$

where V_i , $k_i = 2\pi/\lambda_i$, and λ_i ($i = 1, 2$) are the lattice depth and laser wave vector and wavelength. $x_i(t) = b_i \sin(\omega t)$ is the periodic time-dependent lattice shaking. ω is the lattice-shaking frequency and ϕ is the phase of the second laser. Experimentally, a shaking sinusoidal lattice can be realized through a modulation of the driving frequency and by changing the relative phase of the acousto-optic modulators [46]. Here we assume that the two lattices experience the same shaking amplitude $b = 0.2$, which is within the current experimental technology [46], and describe the two lattice-shaking amounts as $b_1 = b\lambda_1/2$ and $b_2 = b\lambda_2/2$. In the following, we choose the lattice spacing $a = \lambda_1/2 = 1$ and $\hbar = 1$ and assume the first lattice depth V_1 is much bigger than the second lattice depth V_2 . In the absence of lattice shaking $b = 0$, the tight-binding Hamiltonian from Eq. (1) leads to the so-called AA model, which is widely used in the investigation of Anderson localization, as well as some topological phases in cold atomic physics [37–41]. In this paper, we refer the tight-binding model from Eq. (1) with $\theta_i(t) \propto \sin \omega t$ as a periodically driven AA model. Considering a unitary rotation, the Hamiltonian is transferred to a new frame $x \rightarrow x + b_1 \sin(\omega t)$, and it displays

a shaking-induced vector potential,

$$\begin{aligned} H_r &= H_1 + H_2, \\ H_1 &= \frac{(p_x - A_x)^2}{2M} + V_1 \sin^2(k_1 x), \\ H_2 &= V_2 \sin^2(k_2 x - A_\phi + \phi/2), \end{aligned} \quad (2)$$

where the induced vector potentials are $A_x = \alpha_1 \cos(\omega t)$ and $A_\phi = \alpha_2 \sin(\omega t)$, with the amplitudes $\alpha_1 = M\omega b_1$ and $\alpha_2 = k_2(b_2 - b_1)$.

We assume that all the atoms are trapped in the lowest band of the optical lattice; then the Hamiltonian in the second quantization formalism is of the form

$$H = \int dx \Psi^\dagger(x) H_r \Psi(x). \quad (3)$$

Expanding the field operator in terms of the Wannier functions $\Psi(x) = \sum_n c_n w(x - x_n)$, one can omit the constant energy terms and get the tight-binding Hamiltonian

$$\begin{aligned} H &= \sum_n J(t)(c_{n+1}^\dagger c_n + \text{H.c.}) \\ &\quad - \sum_n \Delta \cos(2\pi\beta n - A_\phi + \phi) c_n^\dagger c_n, \end{aligned} \quad (4)$$

where $\beta = k_2/k_1$, $J(t) = \int dx w(x - x_{n+1}) H_1 w(x - x_n)$, $\Delta = \frac{V_2}{2} \int dx w(x) \cos(2k_2 x) w(x)$ and the driving amplitude in A_ϕ has been modified as $\alpha_2 = 2k_2(b_2 - b_1)$. Note that this tight-binding model is the AA model, but with an additional periodic drive contained in the induced gauge potentials A_x, ϕ . Here only the on-site contribution of the second optical lattice is kept because we assume V_1 is much bigger than V_2 .

In order to realize a two-band Chern insulator, we choose $k_1 = 2k_2$, then $\beta = 1/2$. In this case, the odd- and even-number lattice sites feel different on-site energies. We label these two sites as a and b and use them to constitute a pseudospin. By employing Fourier transformation and Peierls substitution, the above Hamiltonian can be rewritten in the momentum space as $H = \sum_k C_k^\dagger \mathcal{H}(k) C_k$, where $C_k = (a_k, b_k)^T$. The Hamiltonian density has the form

$$\mathcal{H}(k) = 2t_x \cos(k_x - A_x) \sigma_x + \Delta \cos(\phi - A_\phi) \sigma_z, \quad (5)$$

where t_x is the bare hopping without time-dependent modulation and $\sigma_{x,y,z}$ are the Pauli matrices spanned by a_k and b_k . In the Gaussian approximation for the Wannier function of the ground state, the hopping rate and the on-site energy can be derived as $t_x = (4/\sqrt{\pi}) V_1^{3/4} E_{R1}^{1/4} \exp(-2\sqrt{V_1/E_{R1}})$ and $\Delta = (V_2/2) \exp(-\beta^2/\sqrt{V_1/E_{R1}})$, where the recoil energies $E_{Ri} = \hbar k_i^2/2M$ ($i = 1, 2$). Interestingly, by associating the laser-induced potential A_ϕ with the vector potential A_y , the on-site energies Δ with twice the hopping rate $2t_y$, and the laser phase ϕ with the quasimomentum k_y , one finds that the above 1D driving model can be mapped into the 2D periodically driven π -flux Harper model. In the following, we show that the original gapless quasienergy spectrum will be driven into the analog of a 2D gapped topological phase.

III. THE EFFECTIVE HAMILTONIAN

The essential feature of the above time-dependent Hamiltonian can be captured by an effective time-independent Hamiltonian. This strategy has been extensively studied recently in periodically driven systems [47–49]. Before using this method to derive the effective Hamiltonian of Eq. (5), we expand the Hamiltonian density $\mathcal{H}(k)$ as

$$\mathcal{H} = \mathcal{H}_0 + \sum_{m=1}^{\infty} (\mathcal{H}_m e^{im\omega t} + \mathcal{H}_{-m} e^{-im\omega t}), \quad (6)$$

where each expanding component \mathcal{H}_m has been modified by the Bessel functions $J_m(\alpha_1, \alpha_2)$ (see Appendix A). Based on the above expanding Hamiltonian, following the strategy in Ref. [49], the effective Hamiltonian of the above equation can be expressed as [50]

$$\mathcal{H}_{\text{eff}} = \mathcal{H}_0 + \frac{1}{\omega} \sum_{m=1}^{\infty} \frac{1}{m} [\mathcal{H}_m, \mathcal{H}_{-m}], \quad (7)$$

where we have omitted high orders of $1/\omega$ [49]. When a high driving frequency ($\omega = 8t_x$) is employed, the contribution of high orders can be safely ignored. In Figs. 1(a) and 1(b), we have numerically demonstrated this point through calculating the modification of the second-order terms on the bulk and edge energy spectrums. The results show that the second-order

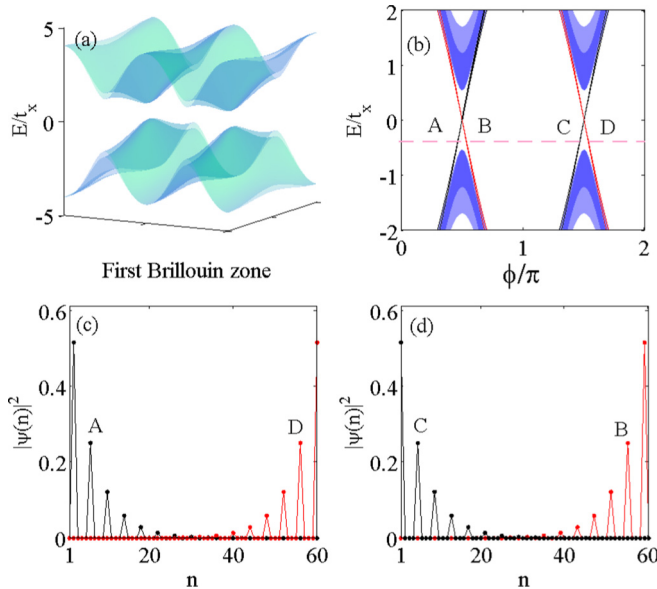


FIG. 1. (Color online) (a) The bulk energy spectrum for a driving AA model. (b) The edge-state spectrum when an open boundary condition in the lattice direction is explored. In both cases, the second-order corrections for Eq. (7) have been calculated and plotted in the shaded spectrum. The dashed line in (b) denotes the Fermi energy $E_f \simeq -0.4t_x$. In this case, there are four edge modes traveling in the gap labeled by A, B, C, and D. We also have plotted the density distribution of the edge modes A and D in (c) and B and C in (d). The results show that the density of edge modes A and D will occupy the b site of each unit cell and the modes B and C will be in the a site of each unit cell. The lattice length is $L = 60$ in the numerical calculation and the other involved parameters are $V_1 = 6E_{R1}$, $V_2 = 0.8E_{R1}$, $b = 0.2$, $t_x \simeq 0.1E_{R1}$, $\omega = 8t_x$, $\Delta = 6t_x$, $\alpha_1 \simeq 0.8$, and $\alpha_2 \simeq 0.6$.

terms only have small influence on the envelope of the spectrum and will not change the gap and the edge spectrum.

In the practical experiment, a weak lattice shaking ($b < 1$) is preferred so that the induced heating on the lattice is small. If the lattice shaking is tuned so that the vector potential amplitudes $\alpha_{1,2} < 1$, one can find that $J_m(\alpha_{1,2}) \sim 10^{-m}$ ($m \geq 3$). In this case, in Eq. (6), only the one- and two-photon transitions dominate the whole dynamics. Then we can write Eq. (6) as

$$\mathcal{H}(k, t) = \mathcal{H}_0 + \sum \mathcal{H}_{m=\pm 1, \pm 2} e^{im\omega t}, \quad (8)$$

where

$$\mathcal{H}_0 = 2t_x J_0(\alpha_1) \cos(k_x) \sigma_x + \Delta J_0(\alpha_2) \cos(\phi) \sigma_z,$$

$$\mathcal{H}_1 = 2t_x J_1(\alpha_1) \sin(k_x) \sigma_x - i \Delta J_1(\alpha_2) \sin(\phi) \sigma_z,$$

$$\mathcal{H}_2 = -2t_x J_2(\alpha_1) \cos(k_x) \sigma_x + \Delta J_2(\alpha_2) \cos(\phi) \sigma_z,$$

$$\mathcal{H}_{-1} = \mathcal{H}_1^\dagger, \quad \mathcal{H}_{-2} = \mathcal{H}_2. \quad (9)$$

By substituting the above equation into Eq. (7), we can obtain an effective two-band Chern insulator model Hamiltonian,

$$\mathcal{H}_{\text{eff}} = h_x \sigma_x + h_y \sigma_y + h_z \sigma_z, \quad (10)$$

where

$$h_x = 2t_x J_0(\alpha_1) \cos(k_x),$$

$$h_y = \frac{8}{\omega} t_x \Delta J_1(\alpha_1) J_1(\alpha_2) \sin(k_x) \sin(\phi), \quad (11)$$

$$h_z = \Delta J_0(\alpha_2) \cos(\phi).$$

As shown before, the above 1D atom-lattice system without shaking can be described by the 2D π -flux model. The x -direction momentum k_x and the laser phase ϕ constitute the 2D space (k_x, ϕ) , which form a 2D torus under the periodic boundary condition along the x direction. In Fig. 1(a), we plot the energy spectrum with driving in the first Brillouin zone of this artificial 2D space $k_x \in [0, \pi]$ and $\phi \in [-\pi, \pi]$. In the absence of shaking, the energy spectrum is gapless and there are two Dirac points, $D_1 = (\frac{\pi}{2}, \frac{\pi}{2})$ and $D_2 = (\frac{\pi}{2}, -\frac{\pi}{2})$. However, when the periodic shaking is applied on the optical lattice, the system will be driven into a gapped insulator phase by the induced y component h_y in Eq. (11).

IV. CHERN INSULATOR AND EDGE STATE

In the following, we show that this gapped phase is indeed a topological insulator state by calculating the Chern number of the occupied ground band and the edge-state spectrum through exploring the open boundary condition. With a unitary rotation, $\sigma_x \rightarrow \sigma_y$, $\sigma_z \rightarrow \sigma_x$, and $\sigma_y \rightarrow \sigma_z$, the above Hamiltonian has the standard form of the Chern insulator model. This rotation communicates with time-reversal symmetry operator and then will not change the topological feature of the original model. Based on a mapping from the Brillouin zone torus (k_x, ϕ) to a spherical surface S^2 , the Chern number of the occupied ground band is expressed as

$$C = \frac{1}{4\pi} \iint dk_x d\phi (\partial_{k_x} \mathbf{h} \times \partial_\phi \mathbf{h}) \cdot \mathbf{h}, \quad (12)$$

where the unit vector field $\mathbf{h} = (h_x, h_y, h_z)/h$, with $h = \sqrt{h_x^2 + h_y^2 + h_z^2}$. The Chern number of this two-band model

can be derived analytically by calculating the sign of the above Jacobian mapping at the two Dirac points [51],

$$C = \frac{1}{2} \sum_{i=1,2} \text{sgn}[(\partial_{k_x} \mathbf{h} \times \partial_{k_y} \mathbf{h}) \cdot \mathbf{h}]|_{D_i}. \quad (13)$$

After substituting Eq. (11) into the above equation, the Chern number of this two-band model can be obtained as

$$C = -\text{sgn}[J_0(\alpha_1)J_0(\alpha_2)]\text{sgn}[J_1(\alpha_1)J_1(\alpha_2)]. \quad (14)$$

Because the shaking amplitude is small in our system, α_1 and α_2 are smaller than 1, the rate of Bessel function is always positive, and the Chern number $C = -1$; thus, the system is in the topological insulator phase. This is quite different from the original gapless semimetal phase without driving.

The appearance of edge state is another hallmark of topological state. To show the behavior of edge state, in Fig. 1(b) we choose the open boundary condition in the x direction and plot the edge state of the energy spectrum when the lattice driving is applied. When a Fermi energy is chosen, there are four gapless edge states traveling in the gap. The velocities of edge modes in the two different edges are opposite. This point can be seen from the spatial density distribution of the four edge modes in Figs. 1(c) and 1(d). The results also show that the density of edge modes A and D will occupy the b site of each unit cell and the modes B and C will stay in the a site of each unit cell. Furthermore, one can find that the density of the edge modes in the region $\phi \in (-\pi/2, \pi/2)$ would always occupy the a -type site in each unit cell, while for other region, the density would occupy the b -type site in each unit cell. This arises from the fact that the eigenstate of our 1D lattice model is the eigenstate of Pauli matrix σ_z . The a - and b -site occupation correspond to the negative and positive eigenstate of σ_z . In the same way, the bulk states also have this feature. This also can explain the topological particle pumping in the next section. Through tuning the laser phase from 0 to 2π , the initial density occupying the b site in each unit cell will shift to the a site of the next unit cell and finally into the b site of this unit cell, which means that the charge will shift by one unit cell.

V. TOPOLOGICAL PARTICLE PUMPING

One of the advantages of the above 1D framework simulating topological phase is that topological pumping can be established naturally. Topological pumping in 1D system was discovered by Thouless [52] and he made the surprising observation that certain band insulators can provide quantized charge transport based on an adiabatic pumping. This topological argument also applies for finite systems coupled to leads [53]. The charge transferred in each pumping cycle is exactly quantized and can be expressed as the Chern number

$$Q = \frac{1}{2\pi} \iint dk_x dt \mathcal{F}(k_x, t) = C[k_x, t], \quad (15)$$

where $C[k_x, t]$ is the Chern number defined on the time and momentum Brillouin zone space, and $\mathcal{F}(k_x, t)$ is the Berry curvature. Topological pumping has also been discussed recently in the context of cold atoms [54–56] and quantum wire systems [57–59].

In the following, we show that the topological pumping can be directly realized based on the proposed 1D framework here. Because our proposed 1D model has the same topological feature as the 2D Chern insulator, its ground state is a topological phase and the corresponding pumping is topologically protected. By slowly tuning the laser phase over one period, the number of the pumping particle number is just the Chern number of the ground band. The number of the pumping particle can be connected with the Wannier center based on the modern charge polarization theory [60]. It states that charge polarization can be related to the Wannier center by

$$P = x_c = \langle \mathcal{W}_n | \hat{x} | \mathcal{W}_n \rangle = \frac{1}{2\pi} \int dk_x A(k_x), \quad (16)$$

where $|\mathcal{W}_n\rangle$ is the Wannier function of the ground band associated with the unit cell n , \hat{x} is the position operator, and $A(k_x)$ is the corresponding Berry connection. If the Hamiltonian H depends on a parameter, the change of the Wannier center with this parameter is a gauge-invariant quantity. In our 1D framework, this parameter is the laser phase. If we tune this phase from $\phi_i = 0$ to $\phi_f = 2\pi$, $H(\phi_i) = H(\phi_f)$, based on Stokes theorem (see Appendix B for details), one can find that the change of the Wannier center for each unit cell is the Chern number of the ground band,

$$\begin{aligned} \Delta x_c &= x_c(\phi_f) - x_c(\phi_i) \\ &= \frac{1}{2\pi} \left[\int dk_x A(k_x, \phi_f) - \int dk_x A(k_x, \phi_i) \right] \\ &= C[k_x, \phi]. \end{aligned} \quad (17)$$

In Fig. 2(a), we have numerically calculated the change of the Wannier center of each lattice site. After tuning the laser phase over one period, the Wannier center for each lattice site will shift downwards two sites (one unit cell); then the Wannier center for each unit cell will shift downwards one. According to the Eq. (17), the total pumping particle number is one and the Chern number is -1 . The sign of the Chern number depends on the shift direction.

Experimentally, the change of Wannier center can be inferred from observing the change of the density distribution along the lattice. The similar method has been proposed recently to detect the Chern number for characterizing integer quantum Hall phase in a 2D optical lattice system [61], where a time-of-flight measurement along the x direction combined with *in situ* detection along the y direction is needed. The atomic density is defined by

$$\rho(\phi, n) = \sum_{E_{oc} \leq E_f} |\psi_{oc}(\phi, n)|^2, \quad (18)$$

where E_f denotes the Fermi energy, E_{oc} denotes the occupied state of the fermionic atoms, and ψ_{oc} is the corresponding wave function. In Fig. 2(b), we have plotted the atomic density distribution along the lattice with the change of the laser phase in the presence of open boundary condition. In the experiment with cold atomic gases, an external harmonic potential is always present to trap the atomic cloud. We have taken its effect into account by adding the term $H_t = V_t \sum_n (n - L/2)^2 c_n^\dagger c_n$ in the numerical calculation, where V_t is the trap strength and L is the lattice size. Indeed, the harmonic trap strength in the experiment can be tuned to small-enough value; the

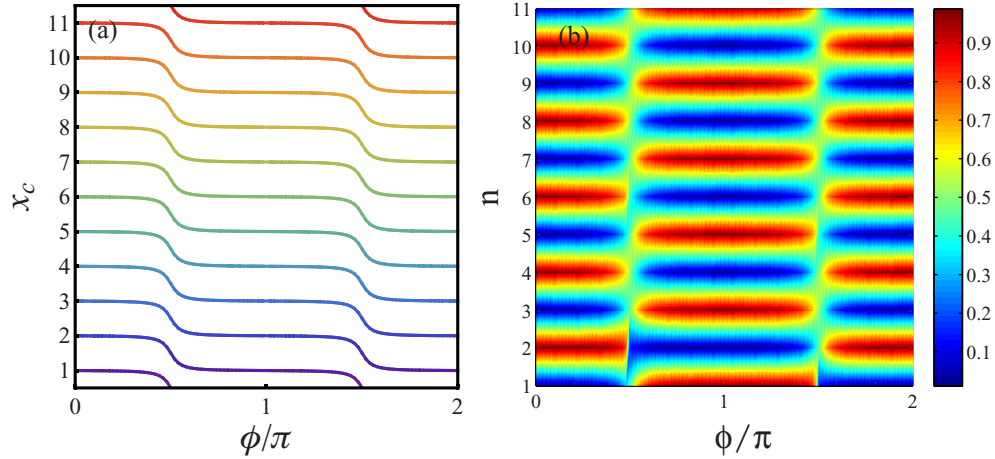


FIG. 2. (Color online) (a) The Wannier center and (b) the atomic density distribution along the optical lattice vary with the laser phase ϕ . After one periodic pumping by tuning the laser phase over one period, the density will shift downwards one unit cell. This phenomenon can be observed in the whole lattice; however, for better illustrating, here we only plot the density distribution of the lattice in a particular range $n \in [1, 11]$. Here the harmonic trap strength $V_t = 0.001$ and other parameters are same with those in Fig. 1.

main results of this paper remain intact in this case. Now we take the lattice site $n = 1$ as an example to describe the particle pumping. When the laser phase is tuned from $\phi = 0$ to $\phi = \pi$, the density will change from $\rho = 0.01$ to $\rho = 0.98$, meaning that the density has been shifted downwards (from the lattice site $n > 1$ to $n = 1$). After tuning the laser phase over one period, the density shifts downwards one unit cell (two lattice sites), which yields the Chern number $C = -1$ and the sign depends on the shift direction. This detection can be done experimentally by tuning the laser phase slowly and performing *in situ* density measurements along the lattice to image the density distribution.

VI. SUMMARY

In summary, we have shown that the topological features of the topological insulator can be simulated and probed with a periodically driven AA model. We realize this 1D model with cold atoms trapped in a 1D shaken optical superlattice. By introducing the laser phase as an additional dimension, we have demonstrated that this 1D model can be mapped into a 2D topological Chern insulator model. The energy spectrum of the system will open a gap even for weak driving. Through calculating the Chern number of the bulk system and the edge states of the system with open boundary condition, we have shown that this gapped state should be a topological insulator state. We have also shown that this 1D framework can form a natural realization of topological pumping and it allows us to directly measure the Chern number of the topological state. This method can be generalized to evanescently coupled helical waveguides for achieving photonic Floquet topological insulators [45], where the time-periodic modulation is replaced with the spatial modulation and the whole topological pumping process can be seen directly in the real space. Interestingly, the above dimension reduction method also provides a new route to simulate the high-dimensional topological phases, including 4D topological insulators. When periodic modulation is applied, it may also allow us to study nonequilibrium topological phases.

ACKNOWLEDGMENTS

F.M. thanks N. Goldman for helpful inputs and revisions. S.L.Z. was supported by the NSFC (Grant No. 11125417), the SKPBR of China (Grant No. 2011CB922104), and the PCSIRT (Grant No. IRT1243). J.B.Y. was supported by the NRF of Singapore (Grant No. WBS: R-710-000-008-271). K.L.C. and R.F. acknowledge support from the National Research Foundation, the Ministry of Education, Singapore.

APPENDIX A: DERIVATION OF EQ. (6)

The periodically driven Hamiltonian density in Eq. (5) can be expanded as $\mathcal{H} = \sum_{n=-\infty}^{\infty} \mathcal{H}_n e^{in\omega t}$ with the Bessel function. This can be seen by first expanding the Hamiltonian as

$$\begin{aligned} \mathcal{H}(k) &= 2t_x \cos(k_x - A_x) \sigma_x + \Delta \cos(\varphi - A_\varphi) \sigma_z \\ &= t_x [e^{ik_x} e^{-i\alpha_1 \cos(\omega t)} + e^{-ik_x} e^{i\alpha_1 \cos(\omega t)}] \sigma_x \\ &\quad + \frac{\Delta}{2} [e^{i\varphi} e^{-i\alpha_2 \sin(\omega t)} + e^{-i\varphi} e^{i\alpha_2 \sin(\omega t)}] \sigma_z. \end{aligned} \quad (\text{A1})$$

Using the Bessel function,

$$\exp\left[\alpha \frac{x - x^{-1}}{2}\right] = \sum_{m=-\infty}^{\infty} J_m(\alpha) x^m, \quad (\text{A2})$$

we can get

$$\begin{aligned} \exp[i\alpha_2 \sin(\omega t)] &= \exp\left[\alpha_2 \frac{e^{i\omega t} - e^{-i\omega t}}{2}\right] \\ &= \sum_{m=-\infty}^{\infty} J_m(\alpha_2) e^{im\omega t}, \\ \exp[i\alpha_1 \cos(\omega t)] &= \exp\left[i\alpha_1 \sin\left(\frac{\pi}{2} + \omega t\right)\right] \\ &= \sum_{m=-\infty}^{\infty} J_m(\alpha_1) e^{im(\frac{\pi}{2} + \omega t)}. \end{aligned} \quad (\text{A3})$$

Through substituting the above equation into Eq. (A1), one can get

$$\mathcal{H} = \mathcal{H}_0 + \sum_{m=1}^{\infty} (\mathcal{H}_m e^{im\omega t} + \mathcal{H}_{-m} e^{-im\omega t}), \quad (\text{A4})$$

where $H_{-m} = H_m^+$. When $m \in \text{odd}$,

$$H_m = x_m \sin k_x \sigma_x - i z_m \sin \varphi \sigma_z, \quad (\text{A5})$$

where the coefficients are

$$\begin{aligned} x_m &= 2 \sin \left(\frac{m\pi}{2} \right) t_x J_m(\alpha_1), \\ z_m &= \Delta J_m(\alpha_2), \end{aligned} \quad (\text{A6})$$

While if $m \in \text{even}$,

$$H_m = x_m \cos k_x \sigma_x + z_m \cos \varphi \sigma_z, \quad (\text{A7})$$

where the coefficient x_m are changed into

$$x_m = 2 \cos \left(\frac{m\pi}{2} \right) t_x J_m(\alpha_1), \quad (\text{A8})$$

and the expression for z_m is same as the odd case.

APPENDIX B: PROOF OF EQ. (17)

The Chern number can be written as a surface integral of the Berry curvature, which is the curl of the Berry connection $\mathbf{A}(k_x, \phi)$ over the first Brillouin zone (FBZ). Naively, it can be recast into a line integral of the Berry connection along the boundary of FBZ via Stokes' theorem,

$$C = \frac{1}{2\pi} \iint_{T^2} dk_x d\phi \nabla \times \mathbf{A}(k_x, \phi) = \frac{1}{2\pi} \oint_{\partial T^2} \mathbf{A}(k_x, \phi) \cdot d\mathbf{l}, \quad (\text{B1})$$

where T^2 and ∂T^2 are the FBZ and its boundary, respectively. However, since the FBZ is a torus which has no boundary, the Chern number is zero if $\mathbf{A}(k_x, \phi)$ is well defined in the whole FBZ. Therefore, nonzero values of the Chern number are the consequences of singularity in the FBZ where the Stokes' theorem is invalid.

Let us assume that the occupied state wave function $\psi(k_x, \phi)$ has a singular point p in the entire FBZ. To apply the Stokes' theorem in this case, we can surround this singular point by a closed loop c_p . On removing this singularity in the wave function, we can use different gauges for $\psi(k_x, \phi)$

inside and outside the loop. Outside the loop, the wave function $\psi(k_x, \phi)$ is well defined; inside the loop, we can do a gauge transform, $\psi \rightarrow e^{if_p} \psi$, to obtain the well-defined wave function. Since the Berry curvature is gauge invariant, this transform does not change the value of the Chern number. However, the Berry connection is indeed gauge variant. In each region, the Berry connections become

$$\begin{aligned} T^2 - s_p : \mathbf{A}(k_x, \phi) &= -i \langle \psi | \nabla | \psi \rangle, \\ s_p : \mathbf{A}_p(k_x, \phi) &= \mathbf{A}(k_x, \phi) + \nabla f_p(k_x, \phi), \end{aligned} \quad (\text{B2})$$

where s_p is the region surrounded by c_p . Because now the Berry connections \mathbf{A} and \mathbf{A}_p are well defined in corresponding regions, we can implement the Stokes' theorem in the following way:

$$\begin{aligned} C &= \frac{1}{2\pi} \left[\iint_{T^2 - s_p} dk_x d\phi \nabla \times \mathbf{A}(k_x, \phi) \right. \\ &\quad \left. + \iint_{s_p} dk_x d\phi \nabla \times \mathbf{A}_p(k_x, \phi) \right] \\ &= \frac{1}{2\pi} \left[\oint_{\partial(T^2 - s_p)} \mathbf{A}(k_x, \phi) \cdot d\mathbf{l} + \oint_{\partial s_p} \mathbf{A}_p(k_x, \phi) \cdot d\mathbf{l} \right] \\ &= \frac{1}{2\pi} \oint_{c_p} [\mathbf{A}_p(k_x, \phi) - \mathbf{A}(k_x, \phi)] \cdot d\mathbf{l}. \end{aligned} \quad (\text{B3})$$

Imagine that c_p expands gradually to the boundary of the FBZ; then, since $\mathbf{A}(k_x, \phi)$ is well defined outside the loop c_p , the line integral is zero. For the connection $\mathbf{A}_p(k_x, \phi)$, it has a singular point outside the loop. We choose a gauge that the singular point of $\mathbf{A}_p(k_x, \phi)$ locates at the boundary of $\phi = 0$ or $\phi = 2\pi$; then using the periodicity of $\mathbf{A}_p(k_x, \phi)$, the Chern number can be further reduced to

$$\begin{aligned} C &= \frac{1}{2\pi} \oint_{c_p} [\mathbf{A}_p(k_x, \phi) - \mathbf{A}(k_x, \phi)] \cdot d\mathbf{l} \\ &= \frac{1}{2\pi} \oint_{\partial T^2} \mathbf{A}_p(k_x, \phi) \cdot d\mathbf{l} \\ &= \frac{1}{2\pi} \left[\int_0^{2\pi} d\phi \mathbf{A}_p(0, \phi) + \int_{2\pi}^0 d\phi \mathbf{A}_p(\pi, \phi) \right. \\ &\quad \left. + \int_0^\pi dk_x \mathbf{A}_p(k_x, 2\pi) + \int_\pi^0 dk_x \mathbf{A}_p(k_x, 0) \right] \\ &= \frac{1}{2\pi} \left[\int_0^\pi dk_x \mathbf{A}_p(k_x, 2\pi) - \int_0^\pi dk_x \mathbf{A}_p(k_x, 0) \right] \\ &= x_c(\phi_f) - x_c(\phi_i) = \Delta x_c. \end{aligned} \quad (\text{B4})$$

-
- [1] M. Z. Hasan and C. L. Kane, *Rev. Mod. Phys.* **82**, 3045 (2010).
 - [2] X.-L. Qi and S.-C. Zhang, *Rev. Mod. Phys.* **83**, 1057 (2011).
 - [3] J. Dalibard, F. Gerbier, G. Juzeliūnas, and P. Öhberg, *Rev. Mod. Phys.* **83**, 1523 (2011); N. Goldman, G. Juzeliūnas, P. Öhberg, and I. B. Spielman, *Rep. Prog. Phys.* **77**, 126401 (2014).
 - [4] N. H. Lindner, G. Refael, and V. Galitski, *Nat. Phys.* **7**, 490 (2011); N. H. Lindner, D. L. Bergman, G. Refael, and V. Galitski, *Phys. Rev. B* **87**, 235131 (2013).

- [5] J.-I. Inoue and A. Tanaka, *Phys. Rev. Lett.* **105**, 017401 (2010); M. Ezawa, *ibid.* **110**, 026603 (2013).
- [6] B. Dora, J. Cayssol, F. Simon, and R. Moessner, *Phys. Rev. Lett.* **108**, 056602 (2012).
- [7] Y. T. Katan and D. Podolsky, *Phys. Rev. Lett.* **110**, 016802 (2013).
- [8] T. Kitagawa, T. Oka, A. Brataas, L. Fu, and E. Demler, *Phys. Rev. B* **84**, 235108 (2011).

- [9] M. Lababidi, I. I. Satija, and Erhai Zhao, *Phys. Rev. Lett.* **112**, 026805 (2014).
- [10] A. G. Grushin, A. Gomez-Leon, and T. Neupert, *Phys. Rev. Lett.* **112**, 156801 (2014).
- [11] T. Kitagawa, E. Berg, M. Rudner, and E. Demler, *Phys. Rev. B* **82**, 235114 (2010).
- [12] M. S. Rudner, N. H. Lindner, E. Berg, and M. Levin, *Phys. Rev. X* **3**, 031005 (2013).
- [13] M. Lewenstein, A. Sanpera, V. Ahufinger, B. Damski, A. Sen De, and U. Sen, *Adv. Phys.* **56**, 243 (2007).
- [14] I. Bloch, J. Dalibard, and W. Zwerger, *Rev. Mod. Phys.* **80**, 885 (2008).
- [15] Y.-J. Lin, R. L. Compton, K. Jimenez-Garcia, J. V. Porto, and I. B. Spielman, *Nature (London)* **462**, 628 (2009); K. Jimenez-Garcia, L. J. LeBlanc, R. A. Williams, M. C. Beeler, A. R. Perry, and I. B. Spielman, *Phys. Rev. Lett.* **108**, 225303 (2012).
- [16] M. Aidelsburger, M. Atala, S. Nascimbene, S. Trotzky, Y.-A. Chen, and I. Bloch, *Phys. Rev. Lett.* **107**, 255301 (2011); M. Aidelsburger, M. Atala, M. Lohse, J. T. Barreiro, B. Paredes, and I. Bloch, *ibid.* **111**, 185301 (2013).
- [17] J. Struck, C. Olschlager, R. Le Targat, P. Soltan-Panahi, A. Eckardt, M. Lewenstein, P. Windpassinger, and K. Sengstock, *Science* **333**, 996 (2011); J. Struck, C. Olschlager, M. Weinberg, P. Hauke, J. Simonet, A. Eckardt, M. Lewenstein, K. Sengstock, and P. Windpassinger, *Phys. Rev. Lett.* **108**, 225304 (2012).
- [18] H. Miyake, G. A. Siviloglou, C. J. Kennedy, W. C. Burton, and W. Ketterle, *Phys. Rev. Lett.* **111**, 185302 (2013).
- [19] Y.-J. Lin, R. L. Compton, K. Jimenez-Garcia, W. D. Phillips, J. V. Porto, and I. B. Spielman, *Nat. Phys.* **7**, 531 (2011).
- [20] P. J. Wang, Z. Q. Yu, Z. K. Fu, J. Miao, L. H. Huang, S. J. Chai, H. Zhai, and J. Zhang, *Phys. Rev. Lett.* **109**, 095301 (2012); L. W. Cheuk, A. T. Sommer, Z. Hadzibabic, T. Yefsah, W. S. Bakr, and M. W. Zwierlein, *ibid.* **109**, 095302 (2012).
- [21] J. Y. Zhang, S. C. Ji, Z. Chen, L. Zhang, Z. D. Du, B. Yan, G. S. Pan, B. Zhao, Y. J. Deng, H. Zhai, S. Chen, and J. W. Pan, *Phys. Rev. Lett.* **109**, 115301 (2012).
- [22] M. C. Beeler, R. A. Williams, K. Jimenez-Garcia, L. J. LeBlanc, A. R. Perry, and I. B. Spielman, *Nature (London)* **498**, 201 (2013); S. L. Zhu, H. Fu, C.-J. Wu, S.-C. Zhang, and L.-M. Duan, *Phys. Rev. Lett.* **97**, 240401 (2006); X. J. Liu, X. Liu, L. C. Kwek, and C. H. Oh, *ibid.* **98**, 026602 (2007).
- [23] L. B. Shao, S. L. Zhu, L. Sheng, D. Y. Xing, and Z. D. Wang, *Phys. Rev. Lett.* **101**, 246810 (2008); C. Wu, *ibid.* **101**, 186807 (2008); D. W. Zhang, Z. D. Wang, and S. L. Zhu, *Front. Phys.* **7**, 31 (2012); F. Mei, D. W. Zhang, and S. L. Zhu, *Chin. Phys. B* **11**, 116106 (2013).
- [24] T. D. Stanescu, V. Galitski, J. Y. Vaishnav, C. W. Clark, and S. Das Sarma, *Phys. Rev. A* **79**, 053639 (2009); T. D. Stanescu, V. Galitski, and S. Das Sarma, *ibid.* **82**, 013608 (2010).
- [25] E. Alba, X. Fernandez-Gonzalvo, J. Mur-Petit, J. K. Pachos, and J. J. Garcia-Ripoll, *Phys. Rev. Lett.* **107**, 235301 (2011); N. Goldman, E. Anisimovas, F. Gerbier, P. Ohberg, I. B. Spielman, and G. Juzeliūnas, *New J. Phys.* **15**, 013025 (2013).
- [26] N. R. Cooper, *Phys. Rev. Lett.* **106**, 175301 (2011).
- [27] X. J. Liu, X. Liu, C. Wu, and J. Sinova, *Phys. Rev. A* **81**, 033622 (2010); X. J. Liu, K. T. Law, and T. K. Ng, *Phys. Rev. Lett.* **112**, 086401 (2014).
- [28] N. Goldman, I. Satija, P. Nikolic, A. Bermudez, M. A. Martin-Delgado, M. Lewenstein, and I. B. Spielman, *Phys. Rev. Lett.* **105**, 255302 (2010).
- [29] B. Beri and N. R. Cooper, *Phys. Rev. Lett.* **107**, 145301 (2011).
- [30] S. L. Zhu, L.-B. Shao, Z. D. Wang, and L.-M. Duan, *Phys. Rev. Lett.* **106**, 100404 (2011); S. Tewari, S. Das Sarma, C. Nayak, C. Zhang, and P. Zoller, *ibid.* **98**, 010506 (2007).
- [31] P. Hauke *et al.*, *Phys. Rev. Lett.* **109**, 145301 (2012); G. C. Liu, N. N. Hao, S. L. Zhu, and W. M. Liu, *Phys. Rev. A* **86**, 013639 (2012); S. K. Baur, M. H. Schleier-Smith, and N. R. Cooper, *ibid.* **89**, 051605 (2014); W. Zheng and H. Zhai, *ibid.* **89**, 061603 (2014); S.-L. Zhang and Q. Zhou, *ibid.* **90**, 051601(R) (2014).
- [32] F. D. M. Haldane, *Phys. Rev. Lett.* **61**, 2015 (1988).
- [33] D. R. Hofstadter, *Phys. Rev. B* **14**, 2239 (1976).
- [34] G. Jotzu *et al.*, *Nature (London)* **515**, 237 (2014).
- [35] M. Aidelsburger *et al.*, [arXiv:1407.4205](https://arxiv.org/abs/1407.4205).
- [36] Y. E. Kraus, Y. Lahini, Z. Ringel, M. Verbin, and O. Zilberberg, *Phys. Rev. Lett.* **109**, 106402 (2012); Y. E. Kraus and O. Zilberberg, *ibid.* **109**, 116404 (2012); M. Verbin, O. Zilberberg, Y. E. Kraus, Y. Lahini, and Y. Silberberg, *ibid.* **110**, 076403 (2013).
- [37] G. Roati *et al.*, *Nature (London)* **453**, 895 (2008); B. Deissler *et al.*, *Nat. Phys.* **6**, 354 (2010); E. Lucioni, B. Deissler, L. Tanzi, G. Roati, M. Zaccanti, M. Modugno, M. Larcher, F. Dalfovo, M. Inguscio, and G. Modugno, *Phys. Rev. Lett.* **106**, 230403 (2011).
- [38] L. J. Lang, X. M. Cai, and S. Chen, *Phys. Rev. Lett.* **108**, 220401 (2012).
- [39] F. Mei, S. L. Zhu, Z. M. Zhang, C. H. Oh, and N. Goldman, *Phys. Rev. A* **85**, 013638 (2012).
- [40] S. L. Zhu, Z.-D. Wang, Y.-H. Chan, and L.-M. Duan, *Phys. Rev. Lett.* **110**, 075303 (2013).
- [41] Z. H. Xu and S. Chen, *Phys. Rev. B* **88**, 045110 (2013).
- [42] P. Marra, R. Citro, and C. Ortix, [arXiv:1408.4457](https://arxiv.org/abs/1408.4457).
- [43] L. Li, Z. H. Xu, and S. Chen, *Phys. Rev. B* **89**, 085111 (2014).
- [44] A. Celi, P. Massignan, J. Ruseckas, N. Goldman, I. B. Spielman, G. Juzeliūnas, and M. Lewenstein, *Phys. Rev. Lett.* **112**, 043001 (2014).
- [45] M. C. Rechtsman¹, J. M. Zeuner, Y. Plotnik, Y. Lumer, D. Podolsky, F. Dreisow, S. Nolte, M. Segev, and A. Szameit, *Nature (London)* **496**, 196 (2013).
- [46] C. V. Parker, L.-C. Ha, and C. Chin, *Nat. Phys.* **9**, 769 (2013).
- [47] A. Gomez-Leon and G. Platero, *Phys. Rev. Lett.* **110**, 200403 (2013); P. Delplace, A. Gomez-Leon, and G. Platero, *Phys. Rev. B* **88**, 245422 (2013); A. Gomez-Leon, P. Delplace, and G. Platero, *ibid.* **89**, 205408 (2014).
- [48] S. Rahav, I. Gilary, and S. Fishman, *Phys. Rev. A* **68**, 013820 (2003).
- [49] N. Goldman and J. Dalibard, *Phys. Rev. X* **4**, 031027 (2014).
- [50] The effective Hamiltonian is equal to the logarithm of the time evolution operator over one driving period, which can be derived through Magnus expansion of the time-ordering evolution operator and making a time average of the time-dependent Hamiltonian over one driving period. However, the initial time in the time average will enter the final effective Hamiltonian. With the method in Refs. [48,49], this dependence can be eliminated through employing two initial and final time-dependent operators before and after the evolution of the effective Hamiltonian. These kick operations are time-periodic and average to zero over one driving period.

- [51] N. A. Usov, *Solid State Commun.* **68**, 943 (1988).
- [52] D. J. Thouless, *Phys. Rev. B* **27**, 6083 (1983).
- [53] P. W. Brouwer, *Phys. Rev. B* **58**, R10135 (1998); M. Buttiker, H. Thomas, and A. Pretre, *Z. Phys. B* **94**, 133 (1994).
- [54] Y. Qian, M. Gong, and C. Zhang, *Phys. Rev. A* **84**, 013608 (2011).
- [55] D. Rossini, M. Gibertini, V. Giovannetti, and R. Fazio, *Phys. Rev. B* **87**, 085131 (2013).
- [56] L. Wang, M. Troyer, and X. Dai, *Phys. Rev. Lett.* **111**, 026802 (2013).
- [57] M. Gibertini, R. Fazio, M. Polini, and F. Taddei, *Phys. Rev. B* **88**, 140508(R) (2013).
- [58] A. Keselman, L. Fu, A. Stern, and E. Berg, *Phys. Rev. Lett.* **111**, 116402 (2013).
- [59] A. Saha, D. Rainis, R. P. Tiwari, and D. Loss, *Phys. Rev. B* **90**, 035422 (2014).
- [60] R. D. King-Smith and D. Vanderbilt, *Phys. Rev. B* **47**, 1651 (1993).
- [61] L. Wang, A. A. Soluyanov, and M. Troyer, *Phys. Rev. Lett.* **110**, 166802 (2013).